



Epitaxial Growth and Luminescent Properties of Mn^{2+} -Activated ZnGa_2O_4 Films

YONG EUI LEE,* DAVID P. NORTON, JOHN D. BUDAI, CHRISTOPHER M. ROULEAU
& JAE-WON PARK

Solid State Division, Oak Ridge National Laboratory, Oak Ridge, TN 37831-6056

Abstract. The epitaxial growth and properties of Mn^{2+} -doped ZnGa_2O_4 thin films on various single crystal substrates using pulsed laser deposition were investigated. Control of Zn/Ga stoichiometry required the use of a mosaic $\text{ZnGa}_2\text{O}_4/\text{ZnO}$ ablation target to compensate for Zn loss due to evaporation. The photoluminescent intensity was a strong function of the Zn/Ga ratio, and also correlated with changes in the surface morphology. Superior photoluminescent intensity was attained from slightly Zn-deficient films which exhibit distinctive worm-like surface features. Enhanced photoluminescent intensity was observed in epitaxial films as compared to randomly-oriented polycrystalline deposits on glass substrates, suggesting an adverse effect of grain boundaries on luminescence properties.

Keywords: pulsed laser deposition, luminescence, epitaxial, $\text{ZnGa}_2\text{O}_4:\text{Mn}$, thin-film phosphors

1. Introduction

Progress in display technology has benefited from continued development of high-performance thin-film phosphor materials for use in field emission displays, thin-film electroluminescent devices, and plasma displays. For these applications, oxide thin film phosphors offer potential advantages over sulfide-based materials due to their good luminescent properties, stability in high vacuum, and absence of corrosive gas emission under electron bombardment [1,2]. Among the oxide phosphors, Mn^{2+} -activated ZnGa_2O_4 is a promising candidate material for green emission. The host material ZnGa_2O_4 has a spinel crystal structure with an energy band gap of about 4.4 eV [3] and shows blue photoluminescence without doping via transition of a self-activated center. The emission shifts to green by activation with Mn^{2+} ions in tetrahedral host lattice sites [4]. The emission band mainly results from the transition ${}^4T_1 \rightarrow {}^6A_1$ of the 3d

electrons in the Mn^{2+} ions (activator) which absorbs transferred energy from host lattice (acting as a sensitizer) in a nonradiative way [5].

Previous work has indicated that as-deposited, randomly-oriented polycrystalline $\text{ZnGa}_2\text{O}_4:\text{Mn}^{2+}$ films on a glass substrate typically do not show appreciable luminescent intensity, requiring a post-annealing process at high temperature to improve the luminescent characteristics. According to the reports on polycrystalline thin-film phosphors, the heat treatment at high temperature enhances the crystallinity of the film resulting in enhanced luminescent intensity. Representative results were reported by Minami et al. [6], in which $\text{ZnO}:\text{Al}/\text{ZnGa}_2\text{O}_4:\text{Mn}$ structures were fabricated on BaTiO_3 ceramic substrates for electroluminescent characterization. Enhanced luminous efficiency was attained from the post-annealed phosphor film, while the as-deposited film exhibited only weak green emission. Hsieh et al. [7] also reported that improved blue cathodoluminescent properties were achieved on heat-treated ZnGa_2O_4 films. These results suggest an interrelation-

*E-mail: yonglee@solid.ssd.ornl.gov.

ship between the structural properties and the luminescent characteristics of the ZnGa_2O_4 phosphor films. A basic understanding of the relationship between the structural and optical luminescent properties of ZnGa_2O_4 films could lead to better performance of thin-film phosphor devices. Unfortunately, there have been few reports focusing on epitaxial luminescent phosphor thin films on single crystal substrates. In this study, we have investigated epitaxial growth and properties of Mn^{2+} -activated ZnGa_2O_4 thin films deposited using pulsed laser ablation. The luminescent properties of epitaxial and polycrystalline films are compared in an attempt to delineate the effects of structural properties on luminescent characteristics.

2. Experimental

A ZnGa_2O_4 ablation target with 2 at.% Mn was prepared by mixing and calcination of ZnO [Alfa, 99.9995%], Ga_2O_3 [Alfa, 99.999%], and MnO_2 [Alfa, 99.999%] powders in air at 1,000°C for 24 hr in covered alumina crucibles. After mixing and pressing, the 1 inch dia. pellets were sintered in air at 1,200°C for 24 hr. 1 inch dia. ZnO pellets were also prepared for mosaic ZnGa_2O_4 :Mn/ZnO ablation targets to control the cation ratio of Zn/Ga in the films. Three different types of targets consisting of: (1) a single ZnGa_2O_4 , (2) the area portion of ZnGa_2O_4 /ZnO of 75/25% (mosaic I) and (3) 50/50% (mosaic II) targets were used. (100) MgO, (100) MgAl_2O_4 , and (100) SrTiO_3 single crystals were used as substrates. Glass substrates were also used to compare the structural

and luminescent properties of epitaxial films with those of polycrystalline films. The films were grown using an excimer KrF laser with a wavelength of 248 nm. The laser fluence was approximately 3.3 J/cm² and the repetition rate used was 5 Hz. Deposition rate was 0.07 nm per shot. Approximately 1 μm thick films were grown at temperatures ranging from 25 to 700°C. Total pressure was fixed at 50 mTorr with various argon (Par) and oxygen partial pressures (PO_2).

Crystal structure and morphology were investigated using X-ray diffraction (XRD) with $\text{CuK}\alpha$ radiation (0.15406 nm wavelength) and atomic force microscopy (AFM) (Digital Instrument Inc.). Compositional analysis was performed by energy dispersive X-ray spectroscopy (EDX). The photoluminescence (PL) spectra were measured at room temperature. Ultraviolet (UV) light radiation with a dominant wavelength of 255 nm was used as an excitation source.

3. Results and Discussion

The cation composition of the films depended strongly on the substrate temperature and target type. Figure 1 shows the dependence of the Zn/Ga ratio in films grown at various substrate temperatures. Higher growth temperatures resulted in a reduction of the Zn/Ga ratio due to higher vapor pressure of Zn as compared with Ga [5]. Using the single ZnGa_2O_4 target, a Zn/Ga ratio of approximately 0.12 was obtained at a deposition temperature of 500°C. To compensate for the loss of Zn in the films, mosaic

Table 1. Summary of processing parameters, structural and luminescent properties of ZnGa_2O_4 :Mn films on single crystal and glass substrates. All films were grown under $\text{PO}_2/P_{\text{Ar}} = 4/46$ mTorr

Substrate	Target ZnGa_2O_4 :Mn/ZnO (areal%)	Temperature (°C)	Lattice constant (nm)	FWHM (degrees) $\Delta\theta_{(004)}$	Integrated PL intensity ($\times 10^5$ counts)	Peak maximum (nm)
(100) MgAl_2O_4	100/0	500	$a = b = 0.8295$ $c = 0.8238$	0.43	3.0	506.5
	100/0	500	$c = 0.8258$	0.58	3.1	508.0
(100) MgO	75/25	500	$c = 0.8293$	0.93	1.7	508.5
		600	$a = b = 0.8325$ $c = 0.827$	0.48	11	508.0
Glass	100/0	500	—	—	1.1	507.0
	75/25	500	—	—	0.7	506.0
		600	—	—	4.2	507.5

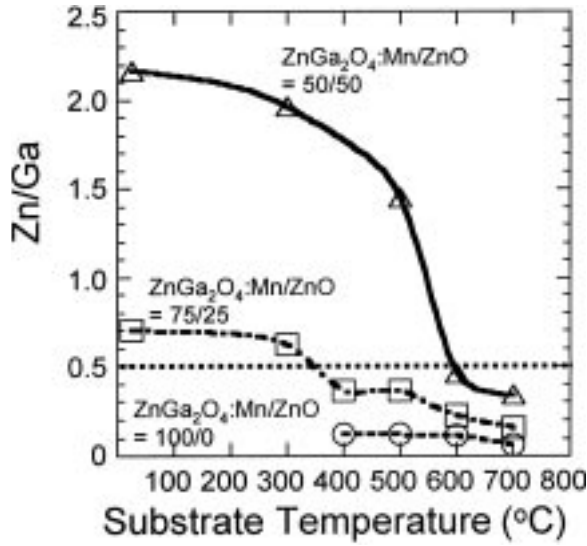


Fig. 1. Compositional variation of Zn/Ga ratio in the ZnGa₂O₄:Mn films deposited with substrate temperatures using various target types.

targets consisting of ZnGa₂O₄:Mn/ZnO with different area portion were used. Compositional analyses on the films grown using the mosaic I and II target shows clearly the substrate temperature dependence of the Zn/Ga ratio in these films as well, with significant Zn deficiency observed at substrate temperatures of 400°C or higher.

Figure 2 shows the X-ray θ - 2θ scans of films grown on (100) MgO single crystal substrates at

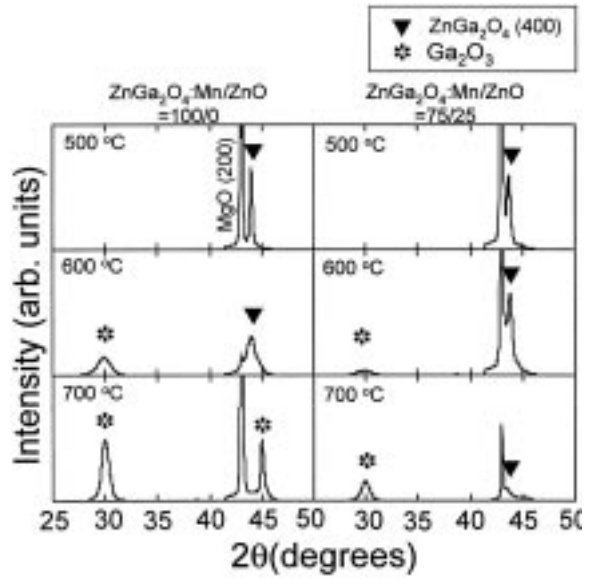


Fig. 2. θ - 2θ x-ray diffraction scan for ZnGa₂O₄:Mn films on (100) MgO substrates under P_{Ar}/P_{O_2} of 46/4 mTorr using a single stoichiometric ZnGa₂O₄:Mn target and a mosaic I target at various substrate temperatures. The mosaic I target consists of ZnGa₂O₄:Mn and ZnO with area portion of 75/25%.

various temperatures using either the 100/0 or 75/25 ZnGa₂O₄:Mn/ZnO mosaic I targets. At 500°C, epitaxial ZnGa₂O₄:Mn films were obtained using either the single or the mosaic I target. At 600°C, a broad diffraction peak at a d-spacing of about 0.3 nm

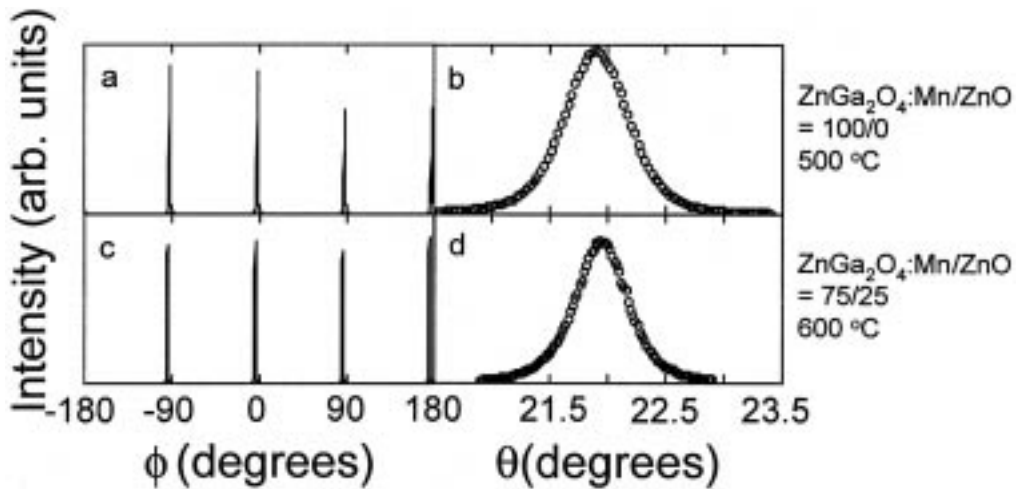


Fig. 3. X-ray ϕ scans for ZnGa₂O₄:Mn films on (100) MgO substrates through (404) (a) at 500°C and using a single target and (c) at 600°C and using a mosaic I target, and corresponding θ scans (b) at 500°C and using a single target and (d) at 600°C and using a mosaic I target. All films were deposited under $P_{Ar}/P_{O_2} = 46/4$ mTorr.

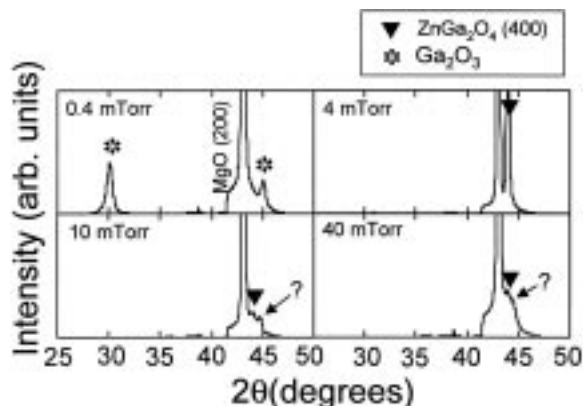


Fig. 4. θ - 2θ x-ray diffraction scan for $\text{ZnGa}_2\text{O}_4:\text{Mn}$ films on (100) MgO substrates at 500°C using a single stoichiometric $\text{ZnGa}_2\text{O}_4:\text{Mn}$ target under different PO_2 . Total pressure was fixed at 50 mTorr.

appears, and the intensity of this peak is higher in the films deposited at 700°C. This peak could be indexed as either (220) ZnGa_2O_4 ($d_{220} = 0.2946$ nm) [8] or (400), (110) Ga_2O_3 ($d_{400} = 0.2967$, $d_{110} = 0.2941$ nm) [9], although it is likely associated with the Ga_2O_3 phase as the peak intensity decreased with increasing Zn/Ga ratio. This peak was not present in the film grown using the mosaic II target at 700°C. The film deposited at 700°C using the single stoichiometric target showed no ZnGa_2O_4 peak, with only the Ga_2O_3 peak present. Amorphous films were obtained at temperatures below 400°C regardless of target types and processing parameters.

To investigate in-plane alignment of the films, X-

ray ϕ scans through the (404) ZnGa_2O_4 peak were performed. The XRD data for films deposited on (100) MgO in Fig. 3 (a) and (c) reveal that the films are in-plane aligned. The films on (100) MgAl_2O_4 and (100) SrTiO_3 single crystal substrates also showed similar results. The Zn/Ga ratio greatly affected the crystallinity of the films as shown in Table 1. In general, a higher Zn content in the target required a higher substrate temperature in order to optimize crystallinity as determined using rocking curves.

The oxygen partial pressure significantly influenced formation of the $\text{ZnGa}_2\text{O}_4:\text{Mn}$ films. Using the stoichiometric target, single phase $\text{ZnGa}_2\text{O}_4:\text{Mn}$ thin films were obtained at $\text{PO}_2 = 4$ mTorr, $T = 500$ °C with a fixed total pressure of 50 mTorr as shown in Fig. 4. Only the Ga_2O_3 peak was observed for the films obtained with $\text{PO}_2 \leq 0.4$ mTorr. Both the ZnGa_2O_4 and Ga_2O_3 peaks decreased significantly in the films deposited with an oxygen partial pressure greater than 4 mTorr.

In addition to crystallinity, the microstructure of the films was also studied using AFM. Figure 5 shows AFM images of the surface morphology for $\text{ZnGa}_2\text{O}_4:\text{Mn}$ films grown at various temperatures on (100) MgO substrates using the mosaic I target. The films deposited at 500 and 700°C show a granular shaped microstructure. In contrast, a distinct worm-like surface microstructure is observed in the film at 600°C. The development of this morphology correlates with the maximum luminescent intensity and may reflect conditions for significant grain growth.

The films exhibited broad-band PL emissions

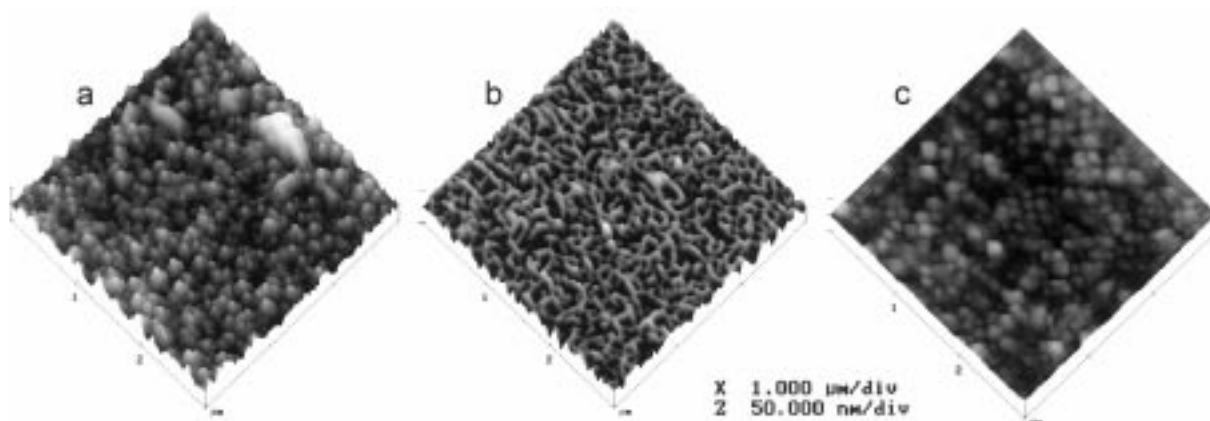


Fig. 5. AFM images of $\text{ZnGa}_2\text{O}_4:\text{Mn}$ films grown on (100) MgO substrates using a mosaic I target at (a) 500°C, (b) 600°C, and (c) 700°C.

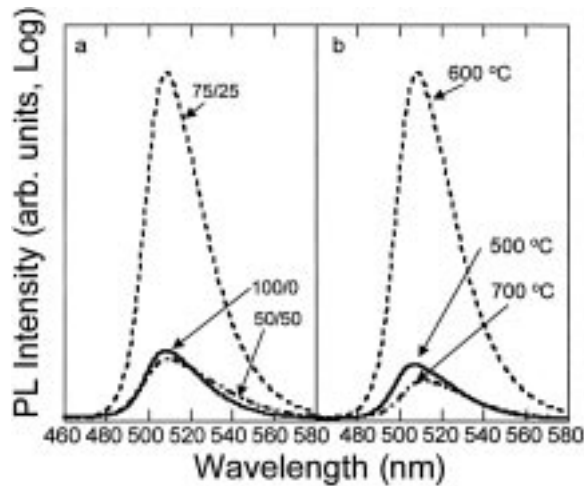


Fig. 6. PL emission spectra from $\text{ZnGa}_2\text{O}_4\text{:Mn}$ films grown on (100) MgO substrates (a) with various target types at 600°C and (b) with various substrate temperatures using a mosaic I target.

extending from 470 to 580 nm with a maximum at 506–512 nm. The PL intensity was dependent strongly upon the growth parameters, including the target type and growth temperature as shown in Fig. 6 and Table 1. Note that both of these parameters strongly affect the Zn/Ga ratio in the films. The results indicate that slightly Zn deficient films ($\text{Zn/Ga} \approx 0.36 - 0.4$) exhibit superior PL intensities over stoichiometric films. Similar results have been reported elsewhere [10,11]. This result is consistent with that reported by Minami et al. [10] in which a maximum luminance of 600 cd/m^2 was obtained for a Zn/Ga ratio of 0.3–0.5 in electroluminescent devices using a $\text{ZnGa}_2\text{O}_4\text{:Mn}$ phosphor. Yu and Lin [11] also found that Zn deficient ZnGa_2O_4 films had excellent cathodoluminescence characteristics and suggested that the excess Ga contents act as the activators for the luminescence. The loss of the Zn in the host lattice may also enhance Mn^{2+} ion substitution on the tetrahedral Zn sites, resulting in enhanced luminescent intensity. It is also possible that Zn vacancies and/or interstitial Ga play an active role in the luminescent process. It is important to note that films deposited on single crystal substrates showed enhanced PL luminescent intensities as compared to randomly oriented polycrystalline

films on glass substrates as shown in Table 1. This suggests that grain boundaries adversely affect the luminescent properties. This effect is currently under further investigation.

4. Conclusions

Mn^{2+} -activated ZnGa_2O_4 thin film phosphors were grown on single crystal substrates. The films deposited using a stoichiometric $\text{ZnGa}_2\text{O}_4\text{:Mn}$ target showed a significant Zn deficiency due to the high vapor pressure of Zn, requiring the use of a mosaic target of $\text{ZnGa}_2\text{O}_4\text{:Mn/ZnO}$ to compensate for Zn loss. Optimized PL intensity was achieved for films with a slight Zn deficiency. This also correlated with a distinct worm-like surface morphology. Epitaxial films also showed enhanced PL properties as compared to randomly oriented polycrystalline films.

Acknowledgment

This research was sponsored by the Oak Ridge National Laboratory, managed by Lockheed Martin Energy Research Corp., for the U.S. Department of Energy, under contract DE-AC05-96OR22464.

References

1. A. Vecht, D.W. Smith, S.S. Chadha, and C.S. Gibbons, *J. Vac. Sci. Technol.*, **B12**, 781 (1994).
2. S. Itoh, M. Yoyoyama, and K. Morimoto, *J. Vac. Sci. Technol.*, **A5**, 3430 (1987).
3. S. Itoh, H. Toki, Y. Sato, K. Morimoto, and T. Kishino, *J. Electrochem. Soc.*, **138**, 1509 (1991).
4. L.E. Shea, R.K. Datta, and J.J. Brown Jr., *J. Electrochem. Soc.*, **141**, 1950 (1994).
5. R.J. Hill, *Physical Vapor Deposition*, Appendix C, Airco, Inc., California (1976).
6. T. Minami, Y. Kuroi, and S. Takata, *J. Vac. Sci. Technol.*, **A14**, 1736 (1996).
7. I.J. Hsieh, K.T. Chu, C.F. Yu, and M.S. Feng, *J. Appl. Phys.*, **76**, 3735 (1994).
8. JCPDS #38-1240.
9. JCPDS #41-1103.
10. T. Minami, T. Maeno, Y. Kuroi, and S. Takata, *Jpn. J. Appl. Phys.*, **34**, L684 (1995).
11. C.F. Yu and P. Lin, *J. Appl. Phys.*, **79**, 7191 (1996).